Eur. Phys. J. C 31, 31–36 (2003)
Digital Object Identifier (DOI) 10.1140/epjc/s2003-01285-2

THE EUROPEAN PHYSICAL JOURNAL C

Multi-ring signatures of the oscillation $\nu_\mu \to \nu_e$ in a water Cherenkov detector

A.E. Asratyan[a], G.V. Davidenko, A.G. Dolgolenko, V.S. Kaftanov, M.A. Kubantsev[b], V.S. Verebryusov

Institute of Theoretical and Experimental Physics, B. Cheremushkinskaya St. 25, Moscow 117259, Russia

Received: 14 April 2003 / Revised version: 19 June 2003 /
Published online: 26 September 2003 –

Abstract. Multi-ring signatures of ν_e appearance via the oscillation $\nu_\mu \to \nu_e$ are formulated for a water Cherenkov detector. These signatures are appropriate for long-baseline neutrino experiments operating at relatively high neutrino energies $E_\nu > 2$ GeV that emphasize the matter effect. The NC background is less for selected multi-ring events than for 1e-like events, and may be directly estimated from the data. Our results suggest that best sensitivity to $\sin^2 2\theta_{13}$ and to the sign of Δm^2_{31} can be reached with baselines over some 6000 km.

1 Introduction

Detecting the oscillation $\nu_\mu \to \nu_e$ in long-baseline accelerator experiments will provide clues to a number of neutrino-mixing parameters: the mixing angle θ_{13}, the sign of the "atmospheric" mass-squared difference Δm^2_{31}, and the CP-violating phase δ_{CP} [1]. The sign of Δm^2_{31} is correlated with that of the asymmetry between the $\nu_\mu \to \nu_e$ and $\bar\nu_\mu \to \bar\nu_e$ probabilities induced by the MSW matter effect [2]; the magnitude of this asymmetry is roughly proportional to E_ν for neutrino energies well below the MSW resonance at some 10–15 GeV. At the same time, a similar asymmetry arising from CP violation only depends on the ratio L/E_ν. Therefore, the two effects can be disentangled by comparing the data for different baselines and energies. In the experiment JHF2K [3] due to start operation by the end of the decade, Super-Kamiokande will be irradiated by a ν_μ beam with $\langle E_\nu \rangle \simeq 0.7 - 0.8$ GeV over a baseline of $L = 295$ km. Likewise, in this paper we discuss using a water Cherenkov detector that offers good e/μ and e/h separation and spectrometry for electrons [4], but assume substantially bigger energy and baseline so as to emphasize the matter effect compared to JHF2K. To be specific, we assume that a neutrino beam from Fermilab is aimed at either of three candidate sites for a Megaton-scale water Cherenkov detector [5]: the Homestake mine in South Dakota ($L = 1280$ km), the San Jacinto mountain in California ($L = 2620$ km), and the Frejus tunnel in France ($L = 6830$ km).

Our foremost task is to formulate the selections of ν_e-induced CC events appropriate for $E_\nu > 2$ GeV, so for simplicity the "solar" mass-squared difference Δm^2_{21} is set to zero thus excluding from the simulation any effects of intrinsic CP violation. Relevant neutrino-mixing parameters are assigned the values consistent with the atmospheric and reactor data [6,7]: $\Delta m^2_{31} = \pm 0.003$ eV^2, $\sin^2 2\theta_{23} = 1$, and $\sin^2 2\theta_{13} = 0.04$ (note that the latter value is some 2.5 times below the upper limit imposed in [7]). The matter effect is estimated in the approximation of uniform matter density [2], taking into account the Earth density profile. The matter-enhanced $\nu_\mu \to \nu_e$ probability for $\Delta m^2_{31} > 0$, that equals the $\bar\nu_\mu \to \bar\nu_e$ probability for $\Delta m^2_{31} < 0$ in the one-Δm^2 approximation, is plotted in Fig. 1 as a function of neutrino energy. For the longest baseline of $L = 6830$ km, the oscillation maximum is at $E_\nu \simeq 7$ GeV which conveniently matches the peak of zero-angle ν_μ flux in the "Medium-Energy" (or PH2me) beam designed for the NuMI–MINOS program [8]. For shorter baselines, we assume the same neutrino beam but in an off-axis configuration that allows to enhance the ν_μ flux at oscillation maximum and to suppress the high-energy tail of the E_ν spectrum [9]. The off-axis angle is selected as $\theta_\nu = 7.7$ and 5.6 mrad [10] for $L = 1280$ and 2620 km, respectively. Shown in the lower panels of Fig. 1 are the (oscillation-free) E_ν spectra of all ν_μ- and ν_e-induced CC events for either site, assuming incident neutrinos.

At neutrino energies below 1 GeV, ν_e appearance can be efficiently detected by selecting 1-ring e-like events of the reaction $\nu_e N \to e^- X$ that is dominated by quasielastics. (Here and in what follows, X denotes a system of hadrons other than the π^0, in which the momenta of all charged particles are below the Cherenkov threshold in water.) The background largely comes from the flavor-blind NC reaction $\nu N \to \nu\pi^0 X$ whose cross section[1] rel-

[a] *Corresponding author.* Tel.: + 7-095-237-0079; Fax: + 7-095-127-0837; E-mail address: asratyan@vitep1.itep.ru

[b] Now at Department of Physics and Astronomy, Northwestern University, Evanston, IL 60208, USA

[1] The cross sections of CC and NC reactions are quoted according to the neutrino-event generator NEUGEN [11]

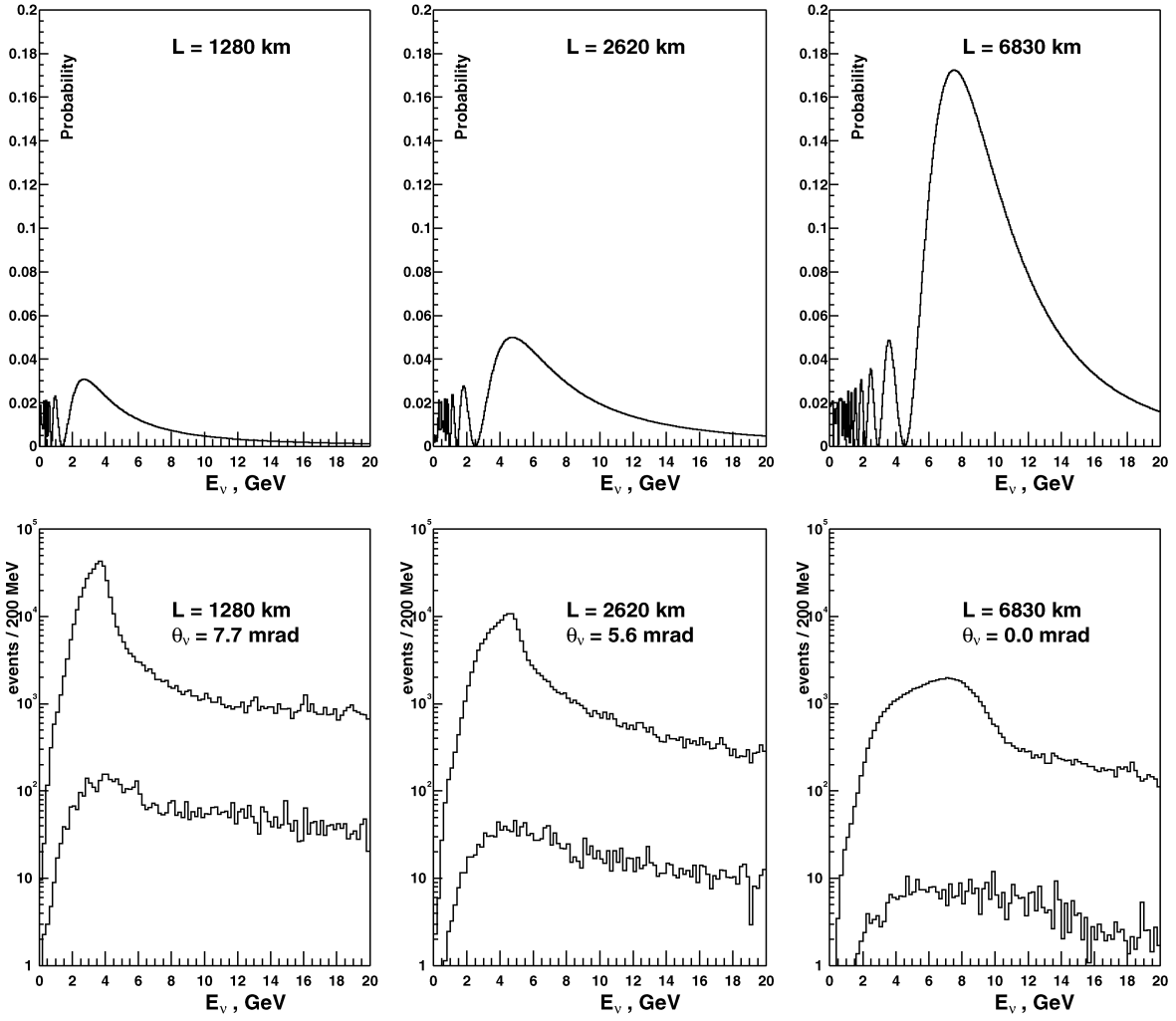

Fig. 1. Top panels: assuming $\Delta m^2_{31} = +0.003$ eV^2, probability of the oscillation $\nu_\mu \to \nu_e$ as a function of neutrino energy for $L = 1280$, 2620, and 6830 km (the left-hand, middle, and right-hand panels, respectively). Bottom panels: oscillation-free E_ν spectra of ν_μ- and ν_e-induced CC events (upper and lower histograms, respectively) for three locations in the medium-energy beam of Fermilab's Main Injector: $L = 1280$ km and $\theta_\nu = 7.7$ mrad (on the left), $L = 2620$ km and $\theta_\nu = 5.6$ mrad (in the middle), and $L = 6830$ km and $\theta_\nu = 0$ (on the right). For incident neutrinos and an exposure of 1 Mton×yr with 1.6×10^{21} p.o.t./yr

ative to $\nu_e N \to e^- X$ increases with E_ν, see Fig. 2. At low neutrino energies ~ 1 GeV, this NC reaction is suppressed by limited phase space and, moreover, the bulk of π^0 mesons are identified by resolving the rings of two photons from $\pi^0 \to \gamma\gamma$ [2]. As a result, in JHF2K the $\nu N \to \nu\pi^0 N$ background is not expected to exceed the "intrinsic" ν_eCC background due to the original ν_e component of the beam [3]. The ν_τCC background, arising from the dominant oscillation $\nu_\mu \to \nu_\tau$ followed by $\nu_\tau N \to \tau^- X$ and $\tau^- \to e^- \nu\bar{\nu}$, is negligibly small due to the threshold effect in τ production. At higher neutrino energies discussed in this paper, the NC reaction $\nu N \to \nu\pi^0 X$ emerges as the dominant source of 1-ring e-like events, and the ν_τCC background tends to exceed the intrinsic ν_eCC background. This is illustrated by the left-hand panel of Fig. 3 showing the $E_{\rm vis}$ distribution of 1e-like events for $\Delta m^2_{31} > 0$, incident neutrinos, and $L = 2620$ km. Depending on the reaction, $E_{\rm vis}$ stands for either the e^- or π^0 energy.

2 The $e\pi^\pm$ and $e\pi^0$ signatures of ν_e appearance

In this paper, we propose to detect the oscillation $\nu_\mu \to \nu_e$ at energies $E_\nu > 2$ GeV by 2- and 3-ring signatures of the reactions $\nu_e N \to e^- \pi^+ X$ and $\nu_e N \to e^- \pi^0 X$ that involve emission of a charged or neutral pion[3]. The motivation is

[2] The efficiency of π^0 reconstruction, as measured in the near detector of the K2K experiment, steeply decreases with increasing π^0 momentum and vanishes at $p(\pi^0) \simeq 900$ MeV [12]

[3] Here and below, corresponding antineutrino reactions are implicitly included

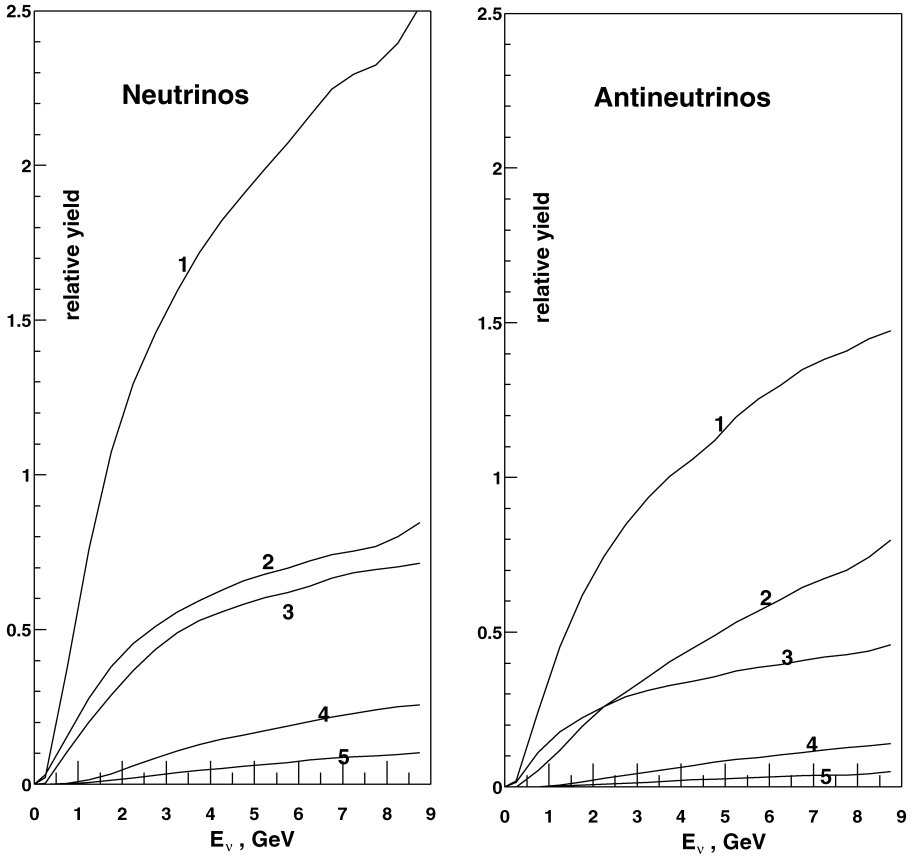

Fig. 2. Cross sections per mean nucleon in water of relevant CC and NC reactions, divided by the $\nu_e N \to e^- X$ cross section, as functions of neutrino energy: $\nu_e N \to e^- \pi^+ X$ (curve 1), $\nu_e N \to e^- \pi^0 X$ (curve 2), $\nu N \to \nu \pi^0 X$ (curve 3), $\nu N \to \nu \pi^0 \pi^\pm X$ (curve 4), and $\nu N \to \nu \pi^0 \pi^0 X$ (curve 5). The left- and right-hand panels are for incident neutrinos and antineutrinos, respectively

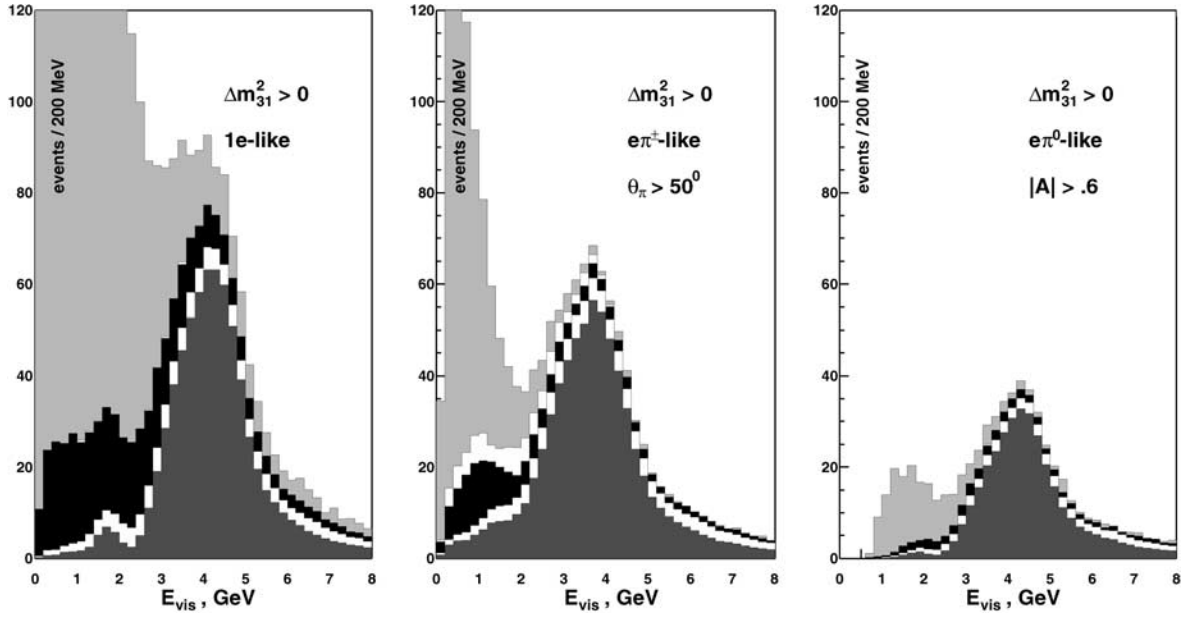

Fig. 3. $E_{\rm vis}$ distributions of 1e-like events (on the left), $e\pi^\pm$-like events (in the middle), and $e\pi^0$-like events (on the right) for $\Delta m^2_{31} > 0$, incident neutrinos, and $L = 2620$ km. From bottom, the depicted components are the $\nu_\mu \to \nu_e$ signal (shaded area), intrinsic ν_eCC background (white area), ν_τCC background (black area), ν_μCC background (white area), and the NC background (light-shaded area). Event statistics are for an exposure of 1 Mton×yr

that, at neutrino energies of a few GeV, the cross section for formation of $\Delta(1232)$ states alone is comparable to quasielastics, whereas the background final states $\nu\pi^0\pi N$ are suppressed with respect to $\nu\pi^0 N$. In other words, one may expect that demanding an extra pion in the final state will effectively reduce the NC background rather

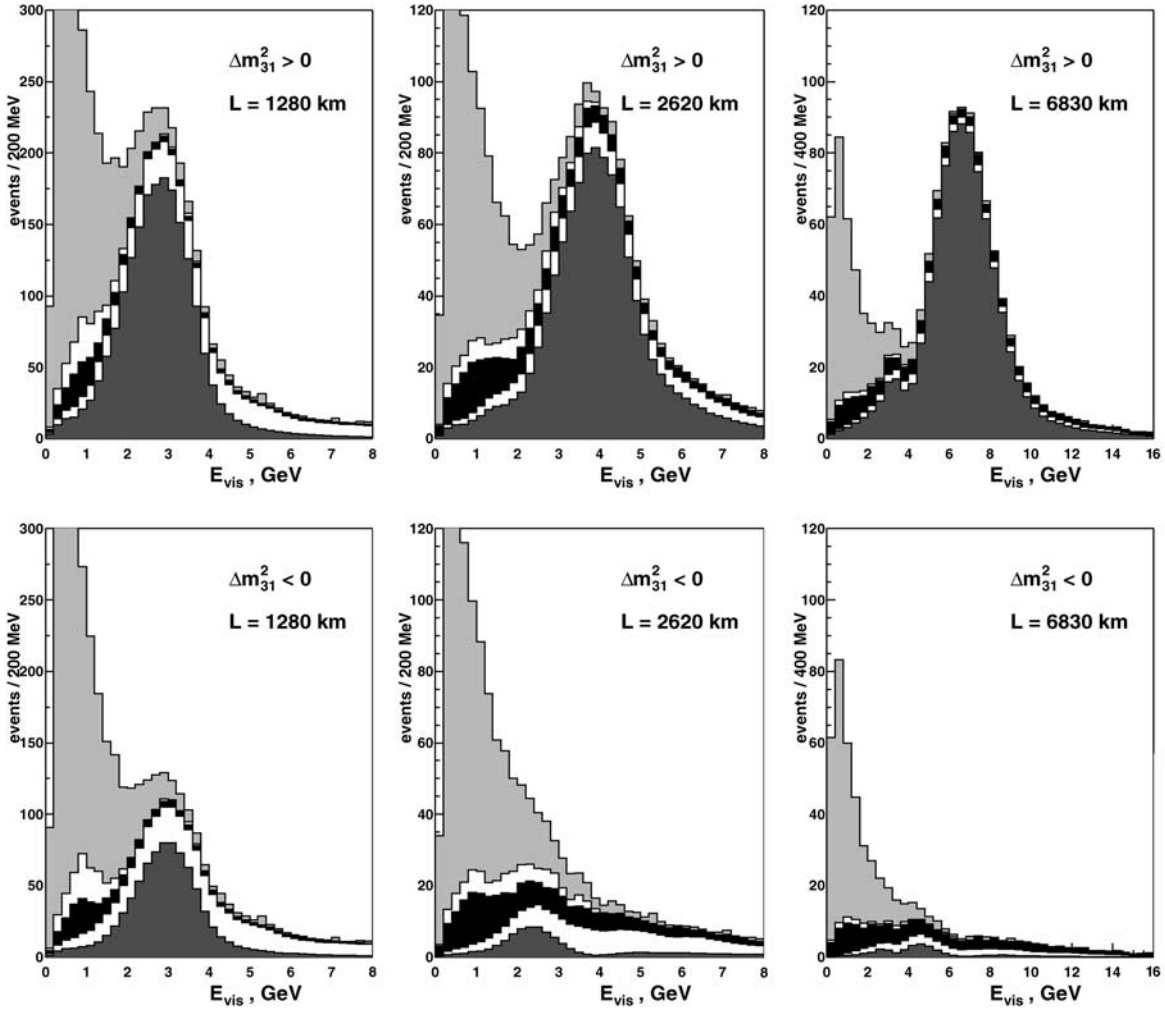

Fig. 4. Combined $E_{\rm vis}$ distributions of $e\pi^{\pm}$- and $e\pi^0$-like events for incident neutrinos and $L = 1280$, 2620, and 6830 km (left-hand, middle, and right-hand panels, respectively). The top and bottom panels are for $\Delta m^2_{31} > 0$ and $\Delta m^2_{31} < 0$. From bottom, the depicted components are the $\nu_\mu \to \nu_e$ signal (shaded area), intrinsic ν_eCC background (white area), ν_τCC background (black area), ν_μCC background (white area), and the NC background (light-shaded area). Event statistics are for an exposure of 1 Mton×yr

than the CC signal. This is illustrated by Fig. 2 showing the cross sections of relevant CC and NC reactions relative to $\nu_e N \to e^- X$ as functions of neutrino energy. The ratios between the cross sections of corresponding CC and NC reactions, $\sigma(\nu_e N \to e^- \pi^+ X)/\sigma(\nu N \to \nu\pi^0\pi^{\pm} X)$ and $\sigma(\nu_e N \to e^- \pi^0 X)/\sigma(\nu N \to \nu\pi^0\pi^0 X)$, are seen to be substantially larger than the ratio $\sigma(\nu_e N \to e^- X)/\sigma(\nu N \to \nu\pi^0 X)$.

The reaction $\nu_e N \to e^- \pi^+ X$ will produce two rings in the detector, of which one is e-like and the other is non-showering. Apart from the reaction $\nu N \to \nu\pi^0\pi^{\pm} X$ with two pions in the final state, a potentially dangerous source of NC background is the more frequent process $\nu p \to \nu\pi^0 p$ in which the momentum of the final proton is above the Cherenkov threshold. Note however that νN kinematics restrict the emission angles of such protons to the region $\cos\theta > 0.45$, whereas pions with momenta above the Cherenkov threshold may even travel in the backward hemisphere. A lower cut on emission angle of the non-showering particle, $\theta > 50^0$, rejects the bulk of visible protons from $\nu p \to \nu\pi^0 p$ [4] and keeps nearly a half of visible pions emitted in the reaction $\nu_e N \to e^- \pi^+ X$. The latter cut will also prevent the π^+ ring from collapsing into the e^- ring. Therefore, we select 2-ring events featuring a e-like ring and an additional ring due to a non-showering particle with a large emission angle of $\theta > 50^0$. This is referred to as the $e\pi^{\pm}$ signature. The distribution of thus selected events in visible energy $E_{\rm vis}$, defined as the energy of the e-like ring, is shown in the middle panel of Fig. 3 for $\Delta m^2_{31} > 0$, incident neutrinos, and $L = 2620$ km. The NC background is seen to be less for the selected $e\pi^{\pm}$-like events than for 1e-like events (compare with the left-hand panel of the same Figure). That the ν_τCC background is also less for $e\pi^{\pm}$-like events than for quasielastics is due to a stronger threshold suppression of $\nu_\tau N \to \tau^- \pi^+ N$

[4] This reaction may also be rejected by identifying relativistic protons by ring shape, as proposed in [13]

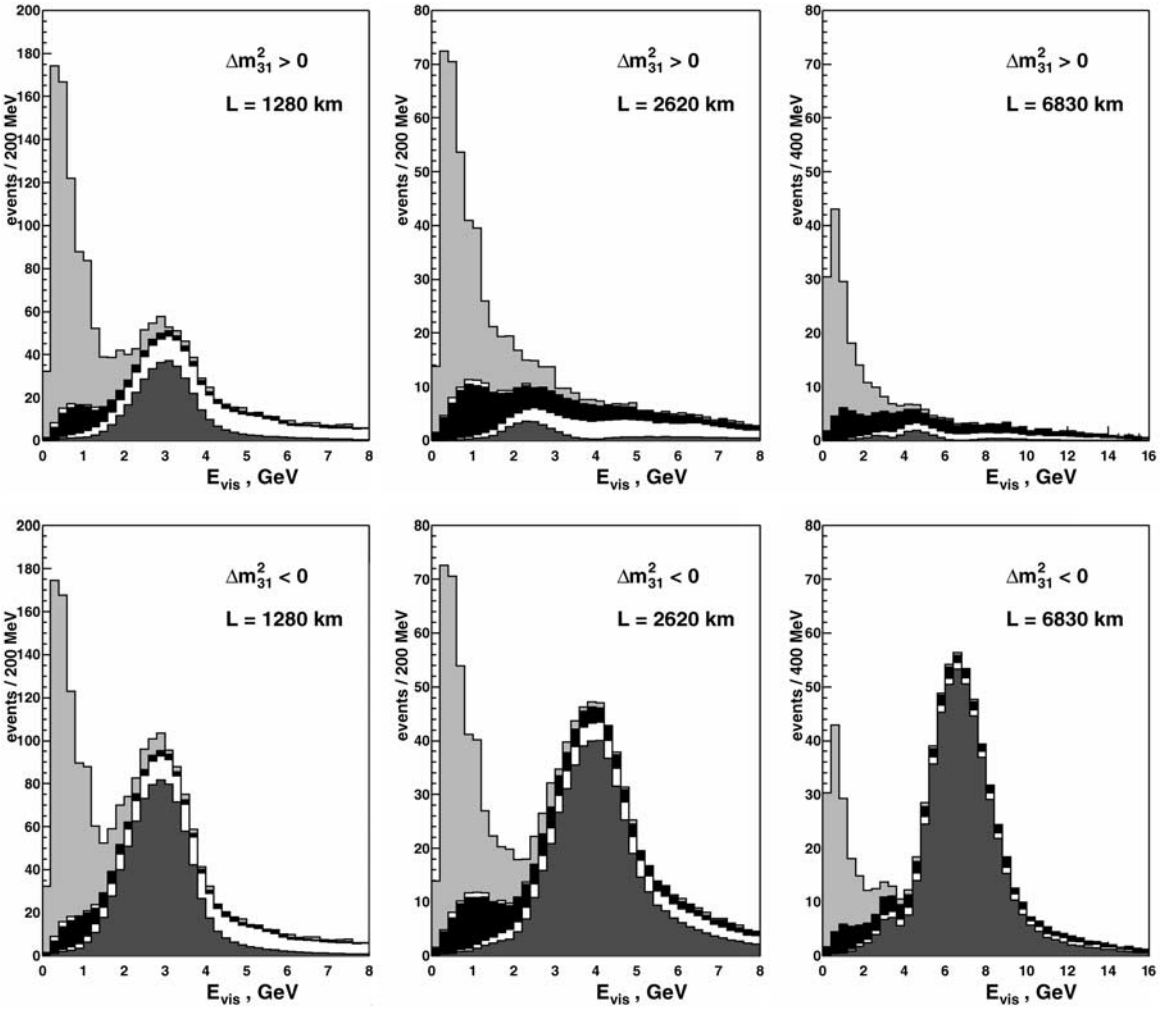

Fig. 5. Same as Fig. 4, but for incident antineutrinos

compared to $\nu_\tau n \to \tau^- p$. On the other hand, the ν_μCC background is negligibly small for 1e-like events, but contributes to selected $e\pi^\pm$-like events through the reaction $\nu_\mu N \to \mu^- \pi^0 X$ in which the muon is emitted at a broad angle.

Next, we consider the reaction $\nu_e N \to e^- \pi^0 X$ that features a neutral pion in the final state[5]. Depending on whether or not the π^0 has been reconstructed, the observable signature is either three e-like rings of which two fit to $\pi^0 \to \gamma\gamma$, or two e-like rings that would not fit to a π^0. The NC background arises from the reaction $\nu N \to \nu\pi^0\pi^0 N$ in which at least one of the two π^0 mesons has not been reconstructed. Note that in the latter reaction the two π^0 mesons are emitted with comparable energies, whereas in $\nu_e N \to e^- \pi^0 X$ the e^- tends to be the leading particle. This suggests a selection based on the absolute value of asymmetry $A = (E_1 - E_2)/(E_1 + E_2)$, where E_1 and E_2 are the energies of the two showers for the two-ring signature, and of the reconstructed π^0 and the "odd" shower—for the three-ring signature. The selection $|A| > 0.6$ has been adopted in this paper. The distribution of thus selected $e\pi^0$-like events in visible energy $E_{\rm vis}$, defined as the total energy of all showers, is shown in the right-hand panel of Fig. 3 for $\Delta m^2_{31} > 0$, incident neutrinos, and $L = 2620$ km. Again, the NC and ν_τCC backgrounds are seen to be less for $e\pi^0$-like than for 1e-like events.

3 Results

Combined $E_{\rm vis}$ distributions of $e\pi^\pm$- and $e\pi^0$-like events, collectively referred to as $e\pi$-like events, are shown in Figs. 4 and 5 for incident neutrinos and antineutrinos and for the three baselines considered. Qualitatively, the signal-to-background ratio for the ν ($\bar\nu$) beam is seen to increase with L as soon as $\Delta m^2_{31} > 0$ ($\Delta m^2_{31} < 0$). This is because corresponding oscillation signals, unlike the background, are progressively matter-enhanced (see Fig. 1). Table 1 lists the total $e\pi$ signals of $\nu_\mu \to \nu_e$ for either sign of Δm^2_{31} and either setting of the beam. Quoted numbers of events refer to an exposure of 1 Mton×yr with 1.6×10^{21} protons on neutrino target per year, as expected upon the

[5] The first observation in a water Cherenkov detector of the corresponding ν_μ-induced reaction, $\nu_\mu N \to \mu^- \pi^0 X$, has been reported in [14]

Table 1. Total $e\pi$ signal of $\nu_\mu \to \nu_e$ and the "figure of merit" $F = S/\sqrt{B}$ for either baseline and beam setting, assuming an exposure of 1 Mton×yr with 1.6×10^{21} p.o.t./yr. The first (second) value corresponds to positive (negative) sign of the mass-squared difference Δm^2_{31}

Baseline	Total signal, ν beam	Total signal, $\bar{\nu}$ beam	F value, ν beam	F value, $\bar{\nu}$ beam
1280 km	1931 (815)	354 (816)	63.0 (27.7)	20.0 (45.5)
2620 km	1021 (89)	38 (487)	52.1 (3.4)	2.4 (39.1)
6830 km	883 (31)	16 (509)	88.4 (2.0)	1.5 (70.3)

planned upgrade of Main Injector's intensity [15]. That the $e\pi$ signals for $L = 2620$ and 6830 km are very similar is a combined effect of matter-induced enhancement, E_ν-dependence of one-pion production, and θ_ν-dependence of neutrino flux. In order to estimate the significance of the $\nu_\mu \to \nu_e$ signal, we vary the $E_{\rm vis}$ interval so as to maximize the quantity $F = S/\sqrt{B}$, where S and B are the numbers of signal and background events falling within the interval. Thus obtained values of F are also quoted in Table 1. These data clearly favor the longest of the three considered baselines. For $L = 6830$ km, the oscillation signal will be largely restricted to the ν data if $\Delta m^2_{31} > 0$, or to the $\bar{\nu}$ data as soon as $\Delta m^2_{31} < 0$.

From statistical errors alone, for $L = 6830$ km we estimate that either the ν or the $\bar{\nu}$ signal will exceed 3σ as soon as $\sin^2 2\theta_{13} > 0.0017$. (A more realistic estimate of sensitivity should of course include the systematic uncertainties [16] which are beyond the scope of this paper.) The reach in $\sin^2 2\theta_{13}$ will be comparable to that of the second phase of JHF2K [3], but ten times higher energy will also allow to probe the sign of Δm^2_{31} through the matter effect.

Note that unlike the $1e$ signature, $e\pi^\pm$ and $e\pi^0$ signatures may allow to estimate the NC background from the data: constraining the axes of all rings to a common point in space will yield the position of the primary vertex. Within errors, this should coincide with the reconstructed vertex of a e^--induced shower, whereas the vertex of an unresolved π^0 shower will be displaced along the shower direction by $\sim \lambda_\gamma$. Here, $\lambda_\gamma \simeq 55$ cm is the mean free path for photons in water. This has to be compared with spatial resolution for the vertex of a single e-like ring, estimated as 34 cm for Super-Kamiokande [4]. Therefore, provided that spatial resolution of the detector is sufficiently high, it may prove possible to directly estimate the NC background by analyzing the displacement of shower vertices from the reconstructed vertex of neutrino collision.

4 Summary

To conclude, we have formulated multi-ring signatures of the oscillation $\nu_\mu \to \nu_e$ in a water Cherenkov detector, that are appropriate for long-baseline neutrino experiments operating at relatively high neutrino energies $E_\nu > 2$ GeV. These emphasize the MSW matter effect and, therefore, may allow to determine the sign of the "atmospheric" mass-squared difference Δm^2_{31}. The NC background is less for selected multi-ring events than for $1e$-like events, and may be directly estimated from the data. Our results suggest that baselines over some 6000 km offer best sensitivity to $\sin^2 2\theta_{13}$ and to the sign of Δm^2_{31}.

Acknowledgements. We wish to thank R. Svoboda for helpful comments and for explaining some details of the water-Cherenkov technique.

References

1. S.M. Bilenky, C. Giunti, W. Grimus, Phys. Rev. D **58**, 033001 (1998); O. Yasuda, Acta Phys. Polon. B **30**, 3089 (1999); H. Minakata, H. Nunokawa, JHEP **10**, 001 (2001); I. Mocioiu, R. Shrock, JHEP **11**, 050 (2001); M. Lindner, TUM-HEP-474/02, arXiv:hep-ph/0209083
2. V. Barger, S. Geer, R. Raja, K. Whisnant, Phys. Rev. D **62**, 013004 (2000); I. Mocioiu, R. Shrock, Phys. Rev. D **62**, 053017 (2000); M. Freund, M. Lindner, S.T. Petcov, A. Romanino, Nucl. Instr. Meth. A **451**, 18 (2000)
3. Y. Itow et al., The JHF–Kamioka neutrino project, KEK Report 2001-4, June 2001, arXiv:hep-ex/0106019; Y. Itow, Nucl. Phys. Proc. Suppl. **112**, 3 (2002)
4. M. Shiozawa, Nucl. Instr. Meth. A **433**, 240 (1999)
5. J.G. Learned, in Proc. 9th Int. Workshop on Neutrino Telescopes, Venice, March 2001, edited by M. Baldo Ceolin, p. 349; C.K. Jung, arXiv:hep-ex/0005046; M. Goodman et al. (UNO Proto-Collaboration), Physics potential and feasibility of UNO, June 2001 (see http://superk.physics.sunysb.edu/)
6. Y. Fukuda et al. (Super-Kamiokande Coll.), Phys. Rev. Lett. **81**, 1562 (1998); T. Kajita, Y. Totsuka, Rev. Mod. Phys. **73**, 85 (2001)
7. M. Apollonio et al. (CHOOZ Coll.), Phys. Lett. B **466**, 415 (1999)
8. S. Wojcicki, Nucl. Phys. Proc. Suppl. **91**, 216 (2001); V. Paolone, Nucl. Phys. Proc. Suppl. **100**, 197 (2001); Neutrino Oscillation Physics at Fermilab: the NuMI–MINOS Project, Fermilab report NuMI-L-375, May 1998 (see http://www.hep.anl.gov/ndk/hypertext/numi_notes.html)
9. D. Beavis et al., BNL-52459, April 1995; A. Para, M. Szleper, Fermilab-PUB-01-324 (2001); S.E. Kopp, arXiv:hep-ex/0210009; D. Ayres et al., arXiv:hep-ex/0210005
10. The ν_μ and ν_e fluxes for these and other off-axis angles may be found at http://www-numi.fnal.gov/fnal_minos/new_initiatives/
11. H. Gallagher, Nucl. Phys. Proc. Suppl. **112**, 188 (2002); H. Gallagher, M. Goodman, Fermilab report NuMI-112, PDK-626, November 1995 (see http://www.hep.anl.gov/ndk/hypertext/numi_notes.html)
12. C. Mauger, Nucl. Phys. Proc. Suppl. **112**, 146 (2002); see extra figures at http://neutrino.kek.jp/nuint01/
13. J.H. Beacom, S. Palomares–Ruiz, hep-ph/0301060
14. S. Mine, Nucl. Phys. Proc. Suppl. **112**, 154 (2002)
15. W. Chou, B. Foster (eds.), Fermilab-TM-2136 (2000) and Fermilab-TM-2169 (2002) (see http://projects.fnal.gov/protondriver/)
16. P. Huber, M. Lindner, W. Winter, Nucl. Phys. B **645**, 3 (2002)